

Resonant slepton production and right sneutrino dark matter in left-right supersymmetry

Mariana Frank¹, Benjamin Fuks^{2,3,4}, Katri Huitu⁵, Santosh Kumar Rai⁶ and Harri Waltari⁵

¹*Department of Physics, Concordia University, 7141 Sherbrooke St. West, Montreal, Quebec, CANADA H4B 1R6*

²*Sorbonne Universités, UPMC Univ. Paris 06, UMR 7589, LPTHE, F-75005 Paris, France*

³*CNRS, UMR 7589, LPTHE, F-75005 Paris, France*

⁴*Institut Universitaire de France, 103 boulevard Saint-Michel, 75005 Paris, France*

⁵*Department of Physics and Helsinki Institute of Physics, University of Helsinki, P.O. Box 64 (Gustaf Hällströmin katu 2), FI-00014 University of Helsinki, Finland,*

⁶*Regional Centre for Accelerator-based Particle Physics, Harish-Chandra Research Institute, HBNI, Chhatnag Road, Jhusi, Allahabad 211019, India.*

E-mail: mariana.frank@concordia.ca, fuks@lpthe.jussieu.fr,

katri.huitu@helsinki.fi, skrai@hri.res.in, harri.waltari@helsinki.fi

ABSTRACT: Right-handed sneutrinos are natural components of left-right symmetric supersymmetric models where the gauge sector is extended to include right-handed weak interactions. Unlike in other models where right-handed sneutrinos are gauge singlets, here the right sneutrino is part of a doublet and could be a dark matter candidate whose annihilation proceeds via gauge interactions. We investigate this possibility, and find that relic density, low-energy observable and direct supersymmetry search constraints can be satisfied when the lightest supersymmetric particle is a right-handed sneutrino. We introduce benchmarks for left-right supersymmetric realizations where either a sneutrino or a neutralino is the lightest superpartner. We then study the LHC signals arising through resonant right-handed slepton production via a W_R gauge-boson exchange that lead to final states enriched in leptons, additionally containing a large amount of missing transverse momentum, and featuring a low jet multiplicity. We find that such a resonant production would boost the chances of discovering these weakly interacting supersymmetric particles for a mass range extending beyond 1 TeV already with a luminosity of 100 fb^{-1} . Finally, we compare sneutrino versus neutralino scenarios, and comment on differences with other sneutrino dark matter models.

KEYWORDS: Supersymmetry phenomenology

Contents

1	Introduction	1
2	A Left-Right Supersymmetric Model with R parity conservation	3
2.1	Model description	3
2.2	Charged sleptons and sneutrinos	6
2.3	Charginos and neutralinos	7
3	Constraints on the spectrum and model parameters	8
3.1	Right-handed gauge sector	8
3.2	The Higgs sector	9
3.3	The neutrino sector	11
3.4	The neutralino and chargino sector	12
3.5	Benchmark point definitions	12
4	Dark matter phenomenology	13
4.1	Sneutrino dark matter	13
4.2	Neutralino dark matter	16
5	Collider phenomenology at the LHC	16
5.1	Analysis strategy for discovering LRSUSY at the LHC	16
5.2	Collider consequences of the LSP nature in LRSUSY models	23
6	Summary and conclusions	23

1 Introduction

While the LHC Run 1 has established the existence of a Higgs boson with properties consistent with those of the Standard Model (SM) one [1, 2] and found no other new particles, the outstanding theoretical problems of the SM remain unresolved. In addition, the existence of dark matter (DM) weighs heavily on the list of experimentally observed but theoretically unexplained problems. One could argue that supersymmetry (SUSY), which provides the best motivated candidate for DM in the lightest supersymmetric particle (LSP), still stands as the best candidate of physics beyond the SM. Unfortunately no signals of supersymmetry have been observed yet, discrediting its simplest incarnation, the constrained minimal supersymmetric standard model (MSSM). In the latter configuration, direct collider bounds push the masses of the strongly interacting supersymmetric partners (gluino and squarks) to be larger than about 1 TeV, which also affects sleptons (their masses being derived from the same universal scalar mass m_0 as the squarks) and electroweak

gauginos (their masses depending on the same universal mass $m_{1/2}$ as the gluino). In addition, the higgsino mass is under pressure from direct searches, leading to a situation in which neutralino DM (either bino- or higgsino-dominated) is in jeopardy. An alternative solution would be to abandon the minimal spectrum of the MSSM and introduce additional symmetries and/or particles which could serve as DM candidates, keeping in mind that SUSY mass limits depend critically on the nature and on the mass of the LSP.

A viable DM alternative has been provided by the sneutrino, which requires the MSSM to be augmented by at least one right-handed (RH) neutrino superfield [3, 4]. The left-handed (LH) sneutrino of the MSSM has a non-zero hypercharge and is thus excluded as a DM candidate. Its coupling to the Z boson indeed causes it to annihilate too much in the early Universe, yielding a relic density much lower than the one measured by the WMAP and Planck satellites [5, 6]. In addition, the presence of a RH neutrino superfield helps in providing a mechanism for generating light neutrino masses which is otherwise absent in the MSSM.

The phenomenology of the MSSM with RH sneutrinos has been investigated in detail, including implications for direct and indirect DM detection, signals at the LHC, and restrictions on the model parameter space [7]. One could also abandon the MSSM formalism and look for extended supersymmetric models, which cure some of the problems that the MSSM inherits from the SM and where the sneutrino emerges as a natural DM candidate [9]. However, most analyses have been performed in the case where the sneutrino is a gauge singlet, which results in LH and RH sneutrino mixings through additional Yukawa and trilinear couplings independent of the LH sneutrinos.

No full investigation exists for the case where RH sneutrinos belong to doublets and the theory possesses a symmetry linking the interactions of the LH and RH fields.* This is the case of the supersymmetric left-right model (LRSUSY) which we propose to investigate here. The LRSUSY model includes three generations of RH neutrino superfields (as parts of RH lepton doublets), and a seesaw as the mechanism for generating the neutrino masses [10] emerges from choosing a triplet representation for the Higgs field responsible for the breaking of the left-right symmetry. The RH neutrino partners are the RH sneutrinos, one of which could be the LSP and thus be a DM candidate. We expect the collider signatures of this model to differ from the cases in which the RH sneutrino is a singlet, as now the sneutrino can couple differently, through gauge interactions.

Left-right supersymmetric models have been explored before [11]. They have several attractive features, such that the fact that they account for neutrino masses, parity violation, disallow explicit R-parity violation, offer a solution to the strong and weak CP violation problems without requiring to introduce an axion [12], and explain the absence of excessive SUSY CP violation. Left-right symmetry is moreover favored by many extra-dimensional models and many gauge unification scenarios, such as $SO(10)$. We shall explore here left-right supersymmetric realizations which, while protecting against spontaneous R -parity

*In Ref. [8], the authors consider a different version of left-right models, where an additional (s)neutrino, singlet under $SU(2)_L$ and $SU(2)_R$, is added. The seesaw mechanism induces a mixing between the left-handed, right-handed, and singlet sneutrinos which can yield the right relic density through Z -channel annihilation.

violation, introduces only one extra singlet superfield. A specific related aspect that has been overlooked so far concerns the possibility of resonantly producing supersymmetric particles at colliders, in particular due to the presence of extra gauge and Higgs bosons. In this context, we explore dark matter constraints and the expected resonant collider signals, paying particular attention to distinguishing features.

Our work is organized as follows. In Sec. 2 we give a description of the model, with a particular emphasis on the slepton, sneutrino, chargino and neutralino sectors. We impose current experimental constraints on the model and define our benchmarks in Sec. 3. We then discuss the phenomenology for cases where the dark matter candidate is either a sneutrino or a neutralino in Sec. 4 and analyze the characteristic signature of this model at the LHC in Sec. 5. Finally, we summarize and conclude our analysis in Sec. 6.

2 A Left-Right Supersymmetric Model with R parity conservation

2.1 Model description

There are several realizations of a left-right symmetry in supersymmetry. In its general formulation, the model is based on the $SU(3)_c \otimes SU(2)_L \otimes SU(2)_R \otimes U(1)_{B-L}$ gauge symmetry. The embedding as a gauge symmetry of the only quantum number left ungauged in the SM, $B - L$ where B and L stand for the baryon and lepton numbers, is an additional attractive feature. The model contains left and right fermion doublets, as well as two sets of gauge bosons lying in the adjoint representation of the $SU(2)_L$ and $SU(2)_R$ groups and a neutral gauge boson connected to $U(1)_{B-L}$. While R -parity, defined as $R_P = (-1)^{3(B-L)+2s}$ (with s being the spin of the particle), is imposed in the MSSM to avoid dangerous baryon and lepton number violating operators, explicit R -parity breaking is forbidden in LRSUSY by the model symmetries. Extra Higgs fields must be introduced to spontaneously break the LRSUSY symmetry group, of which $SU(2)_R$ Higgs triplets consist of the most attractive option as they induce a seesaw mechanism for neutrino mass generation [10]. R -parity may however not be conserved in this setup, this discrete symmetry being broken spontaneously as the vacuum prefers a solution in which the RH sneutrino gets a vacuum expectation value (VEV). Two scenarios have been proposed to remedy this situation. One possibility is to introduce an extra singlet Higgs boson so that a stable R -parity-conserving minimum is found once one-loop corrections are added to the potential [13, 14], while a second option requires to add two new Higgs triplets uncharged under the $B - L$ symmetry $\Omega(1, 3, 1, 0)$ and $\Omega_c(1, 1, 3, 0)$ to break the left-right symmetry spontaneously while conserving R -parity at tree-level [15]. Here we adopt the former, as it is a more minimal realization, for which we present a short description below.

The matter sector of our LRSUSY model contains quark and lepton doublet superfields,

$$\begin{aligned}
 (Q_L)^i &= \begin{pmatrix} u_L^i \\ d_L^i \end{pmatrix} = (\mathbf{3}, \mathbf{2}, \mathbf{1}, \frac{1}{3}) , & (Q_R)^i &= \begin{pmatrix} d_R^i \\ -u_R^i \end{pmatrix} = (\bar{\mathbf{3}}, \mathbf{1}, \mathbf{2}^*, -\frac{1}{3}) , \\
 (L_L)^i &= \begin{pmatrix} \nu_L^i \\ \ell_L^i \end{pmatrix} = (\mathbf{1}, \mathbf{2}, \mathbf{1}, -1) , & (L_R)^i &= \begin{pmatrix} \ell_R^i \\ -\nu_R^i \end{pmatrix} = (\mathbf{1}, \mathbf{1}, \mathbf{2}^*, 1) ,
 \end{aligned} \tag{2.1}$$

where the respective representations under the $SU(3)_c \otimes SU(2)_L \otimes SU(2)_R \otimes U(1)_{B-L}$ gauge symmetry have been indicated. The Higgs sector is in contrast more complicated and features various superfields,

$$\begin{aligned}
\Phi_1 &= \begin{pmatrix} \phi_1^+ & \phi_1^{0'} \\ \phi_1^0 & \phi_1^- \end{pmatrix} = (\mathbf{1}, \mathbf{2}, \mathbf{2}^*, 0) , & \Phi_2 &= \begin{pmatrix} \varphi_2^+ & \varphi_2^0 \\ \varphi_2^{0'} & \varphi_2^- \end{pmatrix} = (\mathbf{1}, \mathbf{2}, \mathbf{2}^*, 0) , \\
\Delta_{1L} &= \begin{pmatrix} \frac{\delta_{1L}^-}{\sqrt{2}} & \delta_{1L}^0 \\ \delta_{1L}^{--} & -\frac{\delta_{1L}^-}{\sqrt{2}} \end{pmatrix} = (\mathbf{1}, \mathbf{3}, \mathbf{1}, -2) , & \Delta_{2L} &= \begin{pmatrix} \frac{\delta_{2L}^+}{\sqrt{2}} & \delta_{2L}^{++} \\ \delta_{2L}^0 & -\frac{\delta_{2L}^+}{\sqrt{2}} \end{pmatrix} = (\mathbf{1}, \mathbf{3}, \mathbf{1}, 2) , \\
\Delta_{1R} &= \begin{pmatrix} \frac{\delta_{1R}^-}{\sqrt{2}} & \delta_{1R}^0 \\ \delta_{1R}^{--} & -\frac{\delta_{1R}^-}{\sqrt{2}} \end{pmatrix} = (\mathbf{1}, \mathbf{1}, \mathbf{3}, -2) , & \Delta_{2R} &= \begin{pmatrix} \frac{\delta_{2R}^+}{\sqrt{2}} & \delta_{2R}^{++} \\ \delta_{2R}^0 & -\frac{\delta_{2R}^+}{\sqrt{2}} \end{pmatrix} = (\mathbf{1}, \mathbf{1}, \mathbf{3}, 2) , \\
S &= (\mathbf{1}, \mathbf{1}, \mathbf{1}, 0) .
\end{aligned} \tag{2.2}$$

The model superpotential is given by

$$\begin{aligned}
W &= (Q_L)^T Y_Q^1 \Phi_1 (Q_R) + (Q_L)^T Y_Q^2 \Phi_2 (Q_R) + (L_L)^T Y_L^1 \Phi_1 (L_R) + (L_L)^T Y_L^2 \Phi_2 (L_R) \\
&+ (L_L)^T Y_L^3 \Delta_{2L} (L_L) + (L_R)^T Y_L^4 \Delta_{1R} (L_R) + S \left[\lambda_L \text{Tr}(\Delta_{1L} \cdot \Delta_{2L}) + \lambda_R \text{Tr}(\Delta_{1R} \cdot \Delta_{2R}) \right. \\
&\left. + \lambda_3 \text{Tr}(\Phi_1^T \tau_2 \Phi_2 \tau_2) + \lambda_4 \text{Tr}(\Phi_1^T \tau_2 \Phi_1 \tau_2) + \lambda_5 \text{Tr}(\Phi_2^T \tau_2 \Phi_2 \tau_2) + \lambda_S S^2 + \xi_F \right] ,
\end{aligned} \tag{2.3}$$

where generation indices are suppressed for clarity. Following the conventions of Ref. [17], the Yukawa couplings Y_Q^j and Y_L^j are 3×3 matrices in flavour space, the λ parameters denote various trilinear Higgs interactions (with τ_2 being the second Pauli matrix) and ξ a linear singlet term. Explicit bilinear supersymmetric Higgs mass terms are in principle allowed by the model symmetries, but we omit them. The bilinear terms are nevertheless dynamically generated when the scalar singlet field S gets a vacuum expectation value.

The left- and right-handed matter superfields and gauge sectors can be related through the parity transformation [12]. Since we may impose parity symmetry on the Lagrangian, the parity violating $\tilde{G}^{\mu\nu} G_{\mu\nu}$ -term is absent and the gluino mass parameter is real. Left-right symmetry further imposes the Yukawa matrices to be Hermitian and the same is true for the soft trilinear terms. The hermiticity of Yukawa matrices also makes the VEVs of the MSSM-like bidoublet Higgses (denoted by v_1, v_2 in the following) real, and hence the model can explain both the strong and SUSY CP problems without introducing the axion as long as the parity breaking scale is not too large [13, 16].

The gauge symmetry is spontaneously broken once the Higgs fields acquire their VEVs,

$$\begin{aligned}
\langle S \rangle &= \frac{v_S}{\sqrt{2}} e^{i\alpha_S} , & \langle \Phi_1 \rangle &= \begin{pmatrix} 0 & \frac{v_1'}{\sqrt{2}} e^{i\alpha_1} \\ \frac{v_1}{\sqrt{2}} & 0 \end{pmatrix} , & \langle \Phi_2 \rangle &= \begin{pmatrix} 0 & \frac{v_2}{\sqrt{2}} \\ \frac{v_2'}{\sqrt{2}} e^{i\alpha_2} & 0 \end{pmatrix} , \\
\langle \Delta_{1R} \rangle &= \begin{pmatrix} 0 & \frac{v_{1R}}{\sqrt{2}} \\ 0 & 0 \end{pmatrix} , & \langle \Delta_{2R} \rangle &= \begin{pmatrix} 0 & 0 \\ \frac{v_{2R}}{\sqrt{2}} & 0 \end{pmatrix} ,
\end{aligned} \tag{2.4}$$

where we assume the LH triplets Δ_{1L}, Δ_{2L} to be inert. This is on one hand motivated by the constraints arising from the ρ parameter and stems on the other hand from the

radiative corrections to the doubly-charged Higgs mass that must be significant enough to satisfy the current experimental bounds. Both these prevent the LH triplet VEVs from being large.

The soft SUSY breaking Lagrangian reads

$$\begin{aligned}
\mathcal{L}_{\text{soft}} = & -\frac{1}{2} \left[M_1 \tilde{B} \tilde{B} + M_{2L} \tilde{W}_L^a \tilde{W}_{La} + M_{2R} \tilde{W}_R^a \tilde{W}_{Ra} + M_3 \tilde{g}^a \tilde{g}_a + \text{h.c.} \right] - m_{\Delta_{1L}}^2 \text{Tr}(\Delta_{1L}^\dagger \Delta_{1L}) \\
& - m_{\Delta_{2L}}^2 \text{Tr}(\Delta_{2L}^\dagger \Delta_{2L}) - m_{\Delta_{1R}}^2 \text{Tr}(\Delta_{1R}^\dagger \Delta_{1R}) - m_{\Delta_{2R}}^2 \text{Tr}(\Delta_{2R}^\dagger \Delta_{2R}) - m_{\Phi_1}^2 \text{Tr}(\Phi_1^\dagger \Phi_1) \\
& - m_{\Phi_2}^2 \text{Tr}(\Phi_2^\dagger \Phi_2) - m_S^2 |S|^2 + m_{\tilde{Q}_L}^2 \tilde{Q}_L^\dagger \tilde{Q}_L - m_{\tilde{Q}_R}^2 \tilde{Q}_R^\dagger \tilde{Q}_R - m_{\tilde{L}_L}^2 (\tilde{L}_L^\dagger \tilde{L}_L) - m_{\tilde{L}_R}^2 (\tilde{L}_R^\dagger \tilde{L}_R) \\
& - \left\{ S [T_L \text{Tr}(\Delta_{1L} \Delta_{2L}) + T_R \text{Tr}(\Delta_{1R} \Delta_{2R}) + T_3 \text{Tr}(\Phi_1^T \tau_2 \Phi_2 \tau_2) + T_4 \text{Tr}(\Phi_1^T \tau_2 \Phi_1 \tau_2) \right. \\
& + T_5 \text{Tr}(\Phi_2^T \tau_2 \Phi_2 \tau_2) + T_S S^2 + \xi_S] + \text{h.c.} \left. \right\} + \left\{ T_Q^1 (\tilde{Q}_L)^T \Phi_1 (\tilde{Q}_R) + T_Q^2 (\tilde{Q}_L)^T \Phi_2 (\tilde{Q}_R) \right. \\
& + T_L^1 (\tilde{L}_L)^T \Phi_1 (\tilde{L}_R) + T_L^2 (\tilde{L}_L)^T \Phi_2 (\tilde{L}_R) + T_L^3 (\tilde{L}_L)^T \Delta_{2L} (\tilde{L}_L) + T_L^4 (\tilde{L}_R)^T \Delta_{1R} (\tilde{L}_R) + \text{h.c.} \left. \right\}, \tag{2.5}
\end{aligned}$$

and includes gaugino mass terms (first bracket), scalar mass terms (the m^2 terms) and trilinear scalar interactions whose strengths are given by the T couplings. For consistency with the superpotential, a linear ξ term has also been introduced.

The v_{iR} , v_1 , v_2 , v'_1 , v'_2 and v_S VEVs can be chosen real and non-negative, while the only complex phases which cannot be rotated away by means of suitable gauge transformations and field redefinitions are denoted by the explicit angles α_1 , α_2 and α_s . However, the CP -violating $W_L^\pm - W_R^\pm$ mixing is proportional to $v_1 v'_1 e^{i\alpha_1}$ and $v_2 v'_2 e^{i\alpha_2}$, and is constrained to be small by $K^0 - \bar{K}^0$ mixing data. To reduce the dimensionality of the parameter space, we therefore assume the hierarchy

$$v_S, v_{1R}, v_{2R} \gg v_2, v_1, v'_1, v'_2 \quad \text{and} \quad v'_1 = v'_2 = \alpha_1 = \alpha_2 = \alpha_S \approx 0. \tag{2.6}$$

This choice originates from the existing constraints on the $SU(2)_R$ gauge bosons that impose the RH VEVs to be large. In the supersymmetric limit, the F -terms and D -terms vanish, when $\lambda_R v_{1R} v_{2R} = \xi_F$ and $v_{1R} = v_{2R}$ [13]. On the other hand, the singlet VEV v_S is induced by the SUSY-breaking linear term ξ_S so that its natural scale is the supersymmetry-breaking scale. We finally realize an ad-hoc hierarchy $v_1, v_2 \gg v'_1, v'_2 \approx 0$ by setting λ_4 and λ_5 and the corresponding SUSY-breaking parameters small. This is a convenient setup where one, for instance, avoids potentially large flavour-changing neutral currents. For further references, we define $\tan \beta = v_2/v_1$ and $\tan \beta_R = v_{2R}/v_{1R}$.

The D -term contribution to the scalar potential (neglecting the squark pieces) is given by

$$\begin{aligned}
V_D = & \sum_i \left[\frac{g_L^2}{8} \left| \text{Tr}(2\Delta_{1L}^\dagger \tau_i \Delta_{1L} + 2\Delta_{2L}^\dagger \tau_i \Delta_{2L} + \Phi_a \tau_i^T \Phi_b^\dagger) + \tilde{L}_L^\dagger \tau_i \tilde{L}_L \right|^2 \right. \\
& + \frac{g_R^2}{8} \left| \text{Tr}(2\Delta_{1R}^\dagger \tau_i \Delta_{1R} + 2\Delta_{2R}^\dagger \tau_i \Delta_{2R} + \Phi_a^\dagger \tau_i^T \Phi_b) + \tilde{L}_R^\dagger \tau_i \tilde{L}_R \right|^2 \left. \right] \\
& + \frac{g_{B-L}^2}{2} \left[\text{Tr}(-\Delta_{1L}^\dagger \Delta_{1L} + \Delta_{2L}^\dagger \Delta_{2L} - \Delta_{1R}^\dagger \Delta_{1R} + \Delta_{2R}^\dagger \Delta_{2R}) - \tilde{L}_L^\dagger \tilde{L}_L + \tilde{L}_R^\dagger \tilde{L}_R \right]^2, \tag{2.7}
\end{aligned}$$

which yields, when expanded around the minimum of the potential, to a coupling between the SM-like Higgs boson and the imaginary parts of RH sneutrino fields. Such a coupling is given, when the small neutrino Yukawa couplings are neglected, by

$$\lambda_{h\tilde{\nu}_{RI}\tilde{\nu}_{RI}} = \frac{1}{4}g_R^2 v \sin(\alpha + \beta) \simeq -\frac{1}{4}g_R^2 v \cos 2\beta, \quad (2.8)$$

where α stands for the mixing angle between the ϕ_1^0 and ϕ_2^0 fields and where the approximated form holds in the alignment limit. This coupling is essential when computing DM annihilation rates in the case of a RH sneutrino LSP. At moderate or large values of $\tan \beta$, $\cos 2\beta \simeq -1$ so that $\lambda_{h\tilde{\nu}_{RI}\tilde{\nu}_{RI}}$ is nearly independent of any free parameter, in particular if we assume $g_R \approx g_L$.

Minimizing the Higgs potential and solving the

$$\frac{\partial V}{\partial v_1} = \frac{\partial V}{\partial v_2} = \frac{\partial V}{\partial v_{1R}} = \frac{\partial V}{\partial v_{2R}} = \frac{\partial V}{\partial v_S} = 0,$$

system of equations, we derive the masses and compositions of the various Higgs bosons. The correct minimum of the potential can however only be evaluated once the one-loop Coleman-Weinberg effective potential

$$V_{\text{eff}}^{1\text{-loop}} = \frac{1}{16\pi^2} \sum_i (-1)^{2s} (2s+1) M_i^4 \left[\ln \left(\frac{M_i^2}{\mu^2} \right) - \frac{3}{2} \right]. \quad (2.9)$$

is included. Without this correction, the minimum would indeed be not phenomenologically acceptable and correspond to the charge-breaking configuration

$$\langle \Delta_{1R} \rangle = \frac{1}{\sqrt{2}} \begin{pmatrix} 0 & v_{1R} \\ v_{1R} & 0 \end{pmatrix}, \quad \langle \Delta_{2R} \rangle = \frac{1}{\sqrt{2}} \begin{pmatrix} 0 & v_{2R} \\ v_{2R} & 0 \end{pmatrix}. \quad (2.10)$$

We refer to and use the results of the recent extensive analysis of Ref. [14] for the calculation of the masses and mixing pattern of the Higgs sector, and focus in the following subsections on the slepton, sneutrino, chargino and neutralino sectors more relevant for this work in which we wish to highlight the possibility for the sneutrino to be the LSP. It is nonetheless equally interesting to look into the phenomenology of the other sectors of the model when a sneutrino LSP is featured. This is left for future work.

2.2 Charged sleptons and sneutrinos

In the interaction basis $(\tilde{L}_L^i, \tilde{L}_R^i)$, the squared-mass matrix for the sleptons is given by

$$\mathcal{M}_L^2 = \begin{pmatrix} m_{\tilde{L}_L}^2 + m_\ell^2 + D_{11} & (T_L^3)_{ij} v \cos \beta + \mu_{\text{eff}} m_\ell \tan \beta \\ (T_L^3)_{ij} v \cos \beta + \mu_{\text{eff}} m_\ell \tan \beta & m_{\tilde{L}_R}^2 + m_\ell^2 + D_{22} \end{pmatrix}, \quad (2.11)$$

where $\mu_{\text{eff}} = \lambda_3 v_s / \sqrt{2}$ and where the D -terms read

$$\begin{aligned} D_{11} &= -\frac{g_L^2}{8} v^2 \cos 2\beta + g_{B-L}^2 (v_{1R}^2 - v_{2R}^2) \quad \text{and} \\ D_{22} &= \frac{g_R^2}{8} [2(v_{1R}^2 - v_{2R}^2) - v^2 \cos 2\beta] - g_{B-L}^2 (v_{1R}^2 - v_{2R}^2). \end{aligned} \quad (2.12)$$

We then extract the scalar and pseudoscalar sneutrino mixing matrices that are of the form

$$\mathcal{M}_\nu^2 = \begin{pmatrix} M_{\tilde{\nu}_L \tilde{\nu}_L}^2 & M_{\tilde{\nu}_L \tilde{\nu}_R}^2 \\ M_{\tilde{\nu}_R \tilde{\nu}_L}^2 & M_{\tilde{\nu}_R \tilde{\nu}_R}^2 \end{pmatrix}. \quad (2.13)$$

In the scalar case, the mass matrix entries are

$$\begin{aligned} M_{\tilde{\nu}_L \tilde{\nu}_L}^2 &= m_{\tilde{L}_L}^2 + D_{11}, \\ M_{\tilde{\nu}_L \tilde{\nu}_R}^2 &= M_{\tilde{\nu}_R \tilde{\nu}_L}^2 = (T_L^2 v - Y_L^2 Y_L^4 v_{1R}) \sin \beta + Y_L^2 \mu_{\text{eff}} \frac{v \cos \beta}{\sqrt{2}}, \\ M_{\tilde{\nu}_R \tilde{\nu}_R}^2 &= m_{\tilde{L}_R}^2 + D_{22} + 2(Y_L^4)^2 v_{1R}^2 - \sqrt{2} T_L^4 v_{1R} + Y_L^4 \lambda_R v_S v_{2R}, \end{aligned} \quad (2.14)$$

where D_{11} and D_{22} are given in Eq. (2.12). The terms depending on the Yukawa couplings Y_L^2 that should have been included within the diagonal blocks have been neglected, as they need to be small to get viable neutrino masses. Moreover, the RH-LH neutrino mixing term will turn to be small as well, unless T_L^2 is large. The pseudoscalar mass matrix entries are given by

$$\begin{aligned} M_{\tilde{\nu}_{IL} \tilde{\nu}_{IR}}^2 &= M_{\tilde{\nu}_{IR} \tilde{\nu}_{IL}}^2 = (T_L^2 v + Y_L^2 Y_L^4 v_{1R}) \sin \beta + Y_L^2 \mu_{\text{eff}} \frac{v \cos \beta}{\sqrt{2}} \\ M_{\tilde{\nu}_{IR} \tilde{\nu}_{IR}}^2 &= m_{\tilde{L}_R}^2 + D_{22} + 2(Y_L^4)^2 v_{1R}^2 + \sqrt{2} T_L^4 v_{1R} - Y_L^4 \lambda_R v_S v_{2R} \end{aligned} \quad (2.15)$$

with $M_{\tilde{\nu}_{IL} \tilde{\nu}_{IL}}^2$ being identical to $M_{\tilde{\nu}_L \tilde{\nu}_L}^2$. Adopting large values for λ_R and a choice of positive parameters implies that the last term of Eq. (2.15) will drive the sneutrino masses. One of the pseudoscalar states, with a flavour aligned with the largest element in the Y_L^4 matrix, will be the LSP unless the corresponding soft supersymmetry breaking mass term is significantly larger than the other terms.

2.3 Charginos and neutralinos

We refer to Ref. [17] for detailed information on the chargino and neutralino sector of the model. We recall below the corresponding mass matrices that will be useful for the design of the benchmark scenarios relevant for this work.

The model has six singly-charged charginos whose associated mass matrix can be written in the $(\tilde{\Delta}_L^\pm, \tilde{\Delta}_R^\pm, \tilde{\Phi}_1^\pm, \tilde{\Phi}_2^\pm, \tilde{W}_L^\pm, \tilde{W}_R^\pm)$ basis as

$$M_{\tilde{\chi}^\pm} = \begin{pmatrix} \lambda_L v_s / \sqrt{2} & 0 & 0 & 0 & 0 & 0 \\ 0 & \lambda_R v_s / \sqrt{2} & 0 & 0 & 0 & -g_R v_{1R} \\ 0 & 0 & 0 & \mu_{\text{eff}} & g_L v_u / \sqrt{2} & 0 \\ 0 & 0 & \mu_{\text{eff}} & 0 & 0 & -g_R v_d / \sqrt{2} \\ 0 & 0 & 0 & g_L v_d / \sqrt{2} & M_{2L} & 0 \\ 0 & g_R v_{2R} & -g_R v_u / \sqrt{2} & 0 & 0 & M_{2R} \end{pmatrix}, \quad (2.16)$$

where $v_u = v \sin \beta$, $v_d = v \cos \beta$.

Although the particle spectrum contains twelve neutralinos, the corresponding mass matrix can be arranged into three block-diagonal pieces when the LH triplet and two neutral

bidoublet Higgs bosons are inert. The first two blocks are expressed, in the $(\tilde{\delta}_{1L}, \tilde{\delta}_{2L})$ and $(\tilde{\phi}_2, \tilde{\varphi}_1)$ bases, as

$$M_{\tilde{\chi}_\delta} = \begin{pmatrix} 0 & \mu_L \\ \mu_L & 0 \end{pmatrix} \quad \text{and} \quad M_{\tilde{\chi}_\Phi} = \begin{pmatrix} 0 & -\mu_{\text{eff}} \\ -\mu_{\text{eff}} & 0 \end{pmatrix}, \quad (2.17)$$

whilst the last block reads, in the $(\tilde{\phi}_1, \tilde{\varphi}_2, \tilde{\delta}_{1R}, \tilde{\delta}_{2R}, \tilde{S}, \tilde{B}, \tilde{W}_L^0, \tilde{W}_R^0)$ basis,

$$M_{\tilde{\chi}^0} = \begin{pmatrix} 0 & -\mu_{\text{eff}} & 0 & 0 & -\mu_d & 0 & \frac{g_L v_u}{\sqrt{2}} & -\frac{g_R v_u}{\sqrt{2}} \\ -\mu_{\text{eff}} & 0 & 0 & 0 & -\mu_u & 0 & -\frac{g_L v_d}{\sqrt{2}} & \frac{g_R v_d}{\sqrt{2}} \\ 0 & 0 & 0 & \mu_R & \frac{\lambda_R v_{2R}}{\sqrt{2}} & g' v_{1R} & 0 & -g_R v_{1R} \\ 0 & 0 & \mu_R & 0 & \frac{\lambda_R v_{1R}}{\sqrt{2}} & -g' v_{2R} & 0 & -g_R v_{2R} \\ -\mu_d & -\mu_u & \frac{\lambda_R v_{2R}}{\sqrt{2}} & \frac{\lambda_R v_{1R}}{\sqrt{2}} & \mu_S & 0 & 0 & 0 \\ 0 & 0 & g' v_R & -g' v_{2R} & 0 & M_1 & 0 & 0 \\ \frac{g_L v_u}{\sqrt{2}} & -\frac{g_L v_d}{\sqrt{2}} & 0 & 0 & 0 & 0 & M_{2L} & 0 \\ -\frac{g_R v_u}{\sqrt{2}} & \frac{g_R v_d}{\sqrt{2}} & -g_R v_{1R} & -g_R v_{2R} & 0 & 0 & 0 & M_{2R} \end{pmatrix}, \quad (2.18)$$

where we have defined $\mu_S = \lambda_S \frac{v_s}{\sqrt{2}}$, $\mu_{L,R} = \lambda_{L,R} \frac{v_s}{\sqrt{2}}$ and $\mu_{u,d} = \lambda_3 \frac{v_{u,d}}{\sqrt{2}}$.

3 Constraints on the spectrum and model parameters

We study in this work the collider signals associated with sneutrino dark matter LRSUSY scenarios at the LHC. As we shall argue in the following, the resonant production of RH sleptons via a W_R -boson exchange is a promising channel. Moreover, the decay chains of heavier superpartners to sneutrinos typically lead to multileptonic final states, and the corresponding SM background is small.

We have computed the particle spectrum with SPHENO-3.3.8 [18], the model files being generated with SARAH [19]. For a reliable computation of the doubly-charged Higgs mass, we have used the dedicated method introduced in Ref. [20]. We have then scanned the parameter space to design our four benchmark scenarios. we describe in the next subsections the constraints that we have imposed and the corresponding phenomenological consequences of our benchmark design strategy.

3.1 Right-handed gauge sector

Unlike in non-supersymmetric left-right symmetric extensions of the SM, predictions for the masses of the right-handed gauge bosons exhibit an upper limit, which depends on the SUSY breaking scale [21, 22], as the charge-conserving vacuum is not stable when $v_R \gg M_{\text{SUSY}}$. However, such a limit does not hold if $B-L=0$ triplets stabilize the vacuum and the right-handed gauge sector is extremely heavy, with masses of $\mathcal{O}(10^{11})$ GeV [15].

Both the ATLAS and CMS collaborations have searched for RH charged and neutral gauge bosons. Current bounds on such additional gauge bosons are derived from both their hadronic and leptonic decay channels [23–27] and are quite strong, the W_R and Z_R masses being constrained to lie above about 2.7 TeV. However, in the LRSUSY setup, the

gauge bosons can easily possess additional decay modes to a pair of lighter supersymmetric particles (usually electroweakinos or sleptons) or to some of the new scalar bosons. All these new modes invariably affect the total decay width and the branching ratios of these gauge bosons so that the existing limits cannot be directly/blindly applied.

We define our benchmark points by setting the branching fraction of the W_R -boson to supersymmetric final states to be of 10–15%, while the total branching ratio into SM final states is fixed to 65–70%. This implies that decays into Higgs states are as well possible. The current bound of 2.7 TeV obtained in the CMS dijet analysis [27] can thus be easily relaxed, the choice $M_{W_R} = 2.7$ TeV being perfectly viable.

We firstly adopt an optimistic benchmark scenario where the W_R -boson mass is close to 2.7 TeV, which gives, since the RH triplet VEV and the Z_R -boson mass are related,

$$M_{W_R} = 2.7 \text{ TeV} , \quad v_R = 5.7 \text{ TeV} \quad \text{and} \quad M_{Z_R} = 4.5 \text{ TeV} . \quad (3.1)$$

We secondly include in our study a more pessimistic benchmark point where the W_R -boson mass is larger,

$$M_{W_R} = 3.5 \text{ TeV} , \quad v_R = 7.5 \text{ TeV} \quad \text{and} \quad M_{Z_R} = 5.9 \text{ TeV} . \quad (3.2)$$

The current LHC bounds on the existence of a Z_R boson [26, 28, 29] are satisfied in both cases.

Eventually, the LHC will probe higher W_R masses. It has been shown that the discovery of W_R bosons with masses reaching up to 5 TeV and their exclusion for masses as large as 6 TeV could be achieved with 300 fb^{-1} of proton-proton collisions at a centre-of-mass energy of $\sqrt{s} = 14$ TeV [30]. Our LRSUSY parameterization allows for stable vacua featuring a heavy W_R boson with a mass ranging of up to about 8 TeV. The total exclusion of W_R bosons predicted in LRSUSY models nevertheless requires a higher collision energy than the one available at the LHC, as there will always remain parts of the parameter space where the W_R boson can escape detection (see also discussion in Sec. 3.2).

3.2 The Higgs sector

In LRSUSY, the doubly-charged Higgs sector plays a central role, not only in terms of the construction of the model, but also for its phenomenology. The doubly-charged Higgs mass matrix has a negative eigenvalue at tree-level once the neutral component of the triplet gets a VEV, and one-loop corrections must be included for stabilizing the scalar potential [13]. The original work relied on the lepton-slepton contributions and hence the couplings of the leptons to the RH triplet Higgs superfield must be taken large for at least one generation. The same couplings however govern the decays of the doubly-charged Higgs boson and it is important to verify the consistency with the various LHC bounds. The latter are strong, with the exception of the case in which the doubly-charged Higgs boson decays into a ditau final-state [31–33]. Such searches have so far managed to push strong bounds on setups where the lightest doubly-charged Higgs boson is of a LH triplet nature. These bounds can be evaded in typical LRSUSY scenarios for RH doubly-charged Higgs bosons, since the associated production of $\delta^{\pm\pm}\delta^\mp$ through W_L^\pm is not possible and in the pair production the

triplet Higgs couples to the Z -boson only through the $B - L$ and W_{3R} components leading to a suppression in the production cross section compared to the left-handed triplets.

Whereas one may assume that the triplet Higgs superfield mostly couples to third generation (s)leptons, non-zero couplings to the other generations are needed to generate masses for the RH neutrinos. In order to evade all doubly-charged Higgs LHC constraints, we fix the model free parameters in a way in which the branching ratio of the doubly-charged Higgs boson into muons and electrons stays below 10%.

Further constraints arise from the sign of the overall one-loop correction to the doubly-charged Higgs mass, which depends on the slepton masses and v_R . If the slepton masses are much smaller than v_R , the correction will be negative and worsen the problem of the negative mass eigenvalue [22]. The large value of v_R that we have adopted hence disfavors a light slepton option. It has however been recently found that the gauge and Higgs sectors can also significantly contribute to the doubly-charged Higgs mass, which opens up a window for lighter RH sleptons and sneutrinos [20].

To obtain a heavy enough doubly-charged Higgs boson, we set the λ_R parameter to a large value, which leads to a large contribution to the doubly-charged Higgs-boson mass from the Higgs sector. We moreover make the electroweakinos rather heavy for benchmarks featuring a sneutrino LSP in order to avoid a neutralino LSP. As mentioned in Sec. 2, we assume that the LH Higgs triplets are inert, so that the corresponding masses are determined by the soft supersymmetry-breaking parameters. Being less relevant for the phenomenology of interest, we set their value larger than 1 TeV.

Whereas in the work of Ref. [20], the highest values for $m_{\Delta^{\pm\pm}}$ turned out to be around 650 GeV, stable vacua can still be achieved with doubly-charged Higgs boson masses slightly above 800 GeV. The projected LHC sensitivity for 100 fb^{-1} of luminosity shows a reach for a potential 3σ discovery that extends up to 950 GeV when the doubly-charged Higgs boson exclusively decays into electrons or muons [34]. The doubly-charged Higgs boson limits stemming from decay modes with tau leptons are not as stringent, due to the efficiency of tau identification. Excluding a 800 GeV doubly-charged Higgs boson decaying solely to same-sign taus would require an improvement of two orders of magnitude with respect to the latest CMS bound [33], which will be challenging even with 3000 fb^{-1} . It is therefore uncertain whether the LHC will be able to exclude the model on the basis of doubly-charged Higgs boson searches only due to the structure of the Yukawa couplings (and the various doubly-charged Higgs boson branching ratios). Moreover, if the vacuum is stabilized by the introduction of $B - L = 0$ triplets, the doubly-charged Higgs boson can be heavier and outside the reach of the LHC. Furthermore, the discovery of a doubly-charged Higgs boson would not be a signal specific to LRSUSY setups and should be used in conjunction with other measurements to draw conclusive LRSUSY statements. The discovery of a doubly-charged scalar field along with doubly-charged higgsinos and a RH gauge boson would be a strong hint towards establishing a left-right supersymmetry without discovering any other SUSY particle, simply by virtue of the robustness of the signal. Such signals have therefore already been studied widely in the literature [35–40], and in this work we focus on another sector of the model.

The upper limit on the tree-level mass of the SM-like Higgs-boson can be much larger

than in the MSSM by the virtue of the extended gauge sector. If $g_L = g_R$, one finds [41]

$$m_h^{\text{tree}} \leq \sqrt{2}m_W \simeq 113.7 \text{ GeV} , \quad (3.3)$$

a value that can be easily lifted to about 125 GeV by incorporating the radiative corrections and by adjusting the stop masses and mixing. The latter depends on $\tan\beta$, and for values close to one, the tree-level mass of the lightest scalar boson tends to vanish, like in the MSSM. However, the LRSUSY D -terms can increase the tree-level Higgs mass beyond values that are typical from the MSSM. Focusing on the rest of the Higgs sector, the second CP -even, the lightest CP -odd and the lightest singly-charged Higgs boson can have masses below or slightly above 1 TeV. Close to the alignment limit, their dominant decay modes involve third generation fermions and the related LHC reach is thus similar as for the heavier states of the MSSM.

We choose a moderate value for $\tan\beta$ so that the bounds stemming from both the direct heavy Higgs-boson searches in the $H/A \rightarrow \tau\tau$ channel [42, 43] are weaker and the contributions to the rare $B_s \rightarrow \mu\mu$ decay are smaller than for large $\tan\beta$. This has an additional advantage to suppress the mixing in the neutral Higgs sector, which may challenge the SM-nature of the lightest state and lead to a large deviation from the SM for the $h \rightarrow b\bar{b}$ branching ratio [14].

Turning to singly-charged Higgs bosons, indirect constraints originating from $b \rightarrow s\gamma$ data [44] suggest that they must be heavy [45], at least if there are no cancellations in the SUSY loop-contributions to the single-charged Higgs-boson mass. This can be accommodated in LRSUSY setups if $\tan\beta_R$ deviates from one and if v_R is large. Such a deviation will subsequently impact one of the diagonal elements of the doubly-charged Higgs mass matrix, making it smaller, and render the task of satisfying the doubly-charged Higgs mass constraints more difficult. We therefore adopt

$$\tan\beta_R \simeq 1.05 , \quad (3.4)$$

which, with our chosen values for v_R , pushes all the MSSM-like Higgs states to be heavier than current LHC bounds. They have masses squared proportional to $g_R^2 v_R^2 (\tan^2\beta_R - 1)$ and are hence at most just above the TeV scale. Moreover, all additional scalar bosons have masses of the order of v_R , v_S , or of the LH triplet soft mass parameters and hence are a lot heavier.

3.3 The neutrino sector

The RH W_R -boson directly decays into RH leptons and neutrinos, provided this decay channel is open. In this case, RH neutrinos could be significantly produced via the resonant production of a W_R -boson, which offers a handle to constrain the masses of the RH neutrinos as a function of the W_R -boson mass. As the RH neutrino subsequently decays through the $N_R \rightarrow \ell W_R^* \rightarrow \ell jj$ channel, the corresponding collider signal ($pp \rightarrow N_R \ell \rightarrow \ell jj$) is made of two charged leptons and two jets, the Majorana nature of the neutrino implying a similar amount of same-sign dilepton and opposite-sign dilepton events [46]. CMS has relied on these considerations to derive simultaneously bounds on the RH neutrinos and

gauge bosons and express them as contours in the (M_{W_R}, M_{N_R}) mass plane, both for the electronic and muonic channels [25]. The bounds are stronger when the neutrino masses lie in the [400 GeV, 1 TeV] mass window, the W_R -boson being constrained to be heavier than 3 TeV. In contrast, for setups with neutrinos lighter than 200 GeV, like in the benchmark scenarios used in this study, the W_R -bosons are instead only constrained by resonance searches in the dijet mode (see Sec. 3.1). We additionally verify that the (weaker) lower bounds extracted from LEP data are fulfilled, which requires the RH Majorana neutrino masses to be above about 90 GeV [47].

As indicated in Sec. 3.2, the doubly-charged Higgs-boson is enforced to decay into an electron or a muon pair with a small branching ratio. This simultaneously drives the RH neutrino masses to low values, as they arise mostly from the Higgs triplet couplings. The lepton-slepton contributions to the doubly-charged Higgs mass cannot however be too negative to ensure that the LHC direct search limits are satisfied, which consequently provides an upper limit on these couplings. We hence set the Yukawa coupling matrix Y_L^4 to be diagonal, and include a hierarchy on the diagonal entries so that the doubly-charged Higgs-boson ditau decay mode is associated with a branching ratio larger than 90%.

3.4 The neutralino and chargino sector

We investigate in this work scenarios in which a sneutrino is a DM candidate, so that neutralinos and charginos must be heavier. The mass of the gaugino-dominated states can be made heavy by setting the corresponding soft masses to large values and we use the singlet superpotential self-coupling λ_S to prevent the singlino-dominated state to be too light and thus the LSP. The higgsino states are in contrast automatically heavy by virtue of the large v_{1R} , v_{2R} and v_S values.

The LHC phenomenology connected to LRSUSY neutralino and chargino states has been recently analysed in Ref. [17], where it has been shown that the leptonic channels are the best probes for LRSUSY neutralinos and charginos. The production rates are in general larger than in the MSSM for not too heavy gauginos, so that this additionally offers handles to distinguish the LRSUSY case from the MSSM. For a comparative study with cases where the neutralino is the LSP, we focus on LRSUSY realizations where the lightest neutralino is bino-dominated. In this case, we fix the bino soft-mass M_1 to a value yielding a DM relic density as measured by the Planck satellite.

3.5 Benchmark point definitions

As mentioned in Sec. 3.1, we consider two sneutrino LSP benchmark points, the first one (BP1) featuring a lighter W_R -boson with $M_{W_R} \simeq 2.7$ TeV, and a second one (BP2) featuring a heavier RH gauge boson with $M_{W_R} \simeq 3.5$ TeV. We additionally define two comparative scenarios BP3 and BP4 where the lightest neutralino is bino-like and the LSP, for the same W_R -boson masses of 2.7 and 3.5 TeV respectively.

We present the values of the most important model parameters in Table 1, as extracted from our scanning procedure, and the relevant part of the particle spectrum in Table 2. The latter also includes the values of several low-energy observables that have been used to constrain the model, enforcing the predictions to agree within two standard deviations

Parameter	Value	Parameter	Value	Parameter	BP1	BP2	BP3	BP4
λ_L	0.4	λ_R	0.9	$\tan \beta$	6.5	8	7	7
λ_S	-0.5	T_R	-2 TeV	$\tan \beta_R$	1.05	1.05	1.04	1.04
T_S	-2 TeV	T_3	1 TeV	v_R (TeV)	5.7	7.5	5.7	7.5
$M_{\Delta 1L, \Delta 2L}^2$	2 TeV ²	M_3	3.5 TeV	v_S (TeV)	7	10	7	8
$(Y_L^4)_{ii}$	(0.019, 0.022, 0.1)	ξ_F	-5000 GeV ²	λ_3	0.15	0.10	0.10	0.08
				$M_{2L,R}$ (GeV)	1200	900	700	700

Table 1. Benchmark scenario definitions. Parameter values common to all benchmark points are shown in the left panel, while benchmark-specific choices are shown in the right panel. We moreover set $\lambda_4 = \lambda_5 = T_L = T_4 = T_5 = 0$ for simplicity.

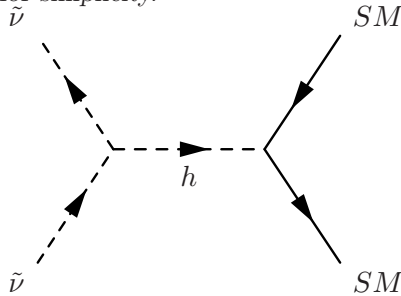


Figure 1. Dominant DM annihilation process for scenarios where the sneutrino is the LSP. The final state generically denotes any SM particle the Higgs boson couples to.

with the current experimental values. Whereas we only list the masses for the three lightest neutralino states, the next two lightest neutralinos are nearly degenerate in mass with the $\tilde{\chi}_3^0$ neutralino. In the BP1 case, the four lightest states are all higgsino-dominated and the fifth one is bino-dominated, whereas for the other benchmark points, the bino-dominated state is the lightest and the next four neutralinos are higgsino-dominated.

4 Dark matter phenomenology

In this section, we respectively focus on scenarios where the LSP is a sneutrino (Sec. 4.1) and a neutralino (Sec. 4.2). We explore the impact of small deviations from the benchmarks introduced in the previous section on the dark matter relic density and investigate how well this agrees with the observed value [6],

$$\Omega_{\text{DM}} h^2 = 0.1198 \pm 0.0015, \quad (4.1)$$

Ω_{DM} being as usual the dark matter energy density evaluated relatively to the critical energy density of the universe and h the reduced Hubble parameter. We additionally investigate the robustness of the direct DM detection bounds as a function of the model parameters.

4.1 Sneutrino dark matter

If the particle spectrum is such that there is no DM co-annihilation channels significantly relevant, sneutrino LSP mostly annihilates via a SM-like Higgs-boson exchange in the s -

Particle	BP1	BP2	BP3	BP4
h	125.2	125.5	124.8	125.3
H_2	551.1	748.5	492.4	657.9
H_3	1958	2076	1949	2363
A_1	551.1	748.5	492.4	657.9
H_1^\pm	563.7	757.7	506.0	668.1
$H_1^{\pm\pm}$	339.1	494.6	431.7	509.8
W_R^\pm	2668	3510	2668	3510
Z'	4476	5889	4476	5889
ν_{Re}	104.2	136.8	104.7	137.6
$\nu_{R\mu}$	120.7	158.4	121.2	159.2
$\nu_{R\tau}$	548.5	719.6	550.8	724.1
$\tilde{\nu}_{I\tau}$	266.5	271.6	416.0	299.7
$\tilde{\nu}_{Ie}$	813.8	663.6	632.2	896.3
$\tilde{\nu}_{I\mu}$	856.9	716.2	792.0	947.3
$\tilde{\nu}_{Re}$	1301	1454	1159	1488
$\tilde{\nu}_{R\mu}$	1331	1566	1312	1590
$\tilde{\nu}_{R\tau}$	2262	2983	2269	2742
\tilde{e}_R	931.7	813.8	773.3	1011
$\tilde{\mu}_R$	931.7	928.2	947.3	1105
$\tilde{\tau}_R$	1399	1837	1449	1678
$\tilde{\chi}_1^0$	731.1	609.8	61.9	62.4
$\tilde{\chi}_2^0$	750.6	711.3	486.6	447.2
$\tilde{\chi}_3^0$	750.9	716.3	501.1	459.3
$\tilde{\chi}_1^\pm$	744.0	703.7	487.5	447.8
$\text{BR}(b \rightarrow s\gamma)$	3.04×10^{-4}	3.10×10^{-4}	3.03×10^{-4}	3.08×10^{-4}
$\text{BR}(B_s \rightarrow \mu\mu)$	2.74×10^{-9}	3.68×10^{-9}	3.44×10^{-9}	2.71×10^{-9}
Δa_μ	1.2×10^{-10}	1.5×10^{-10}	2.1×10^{-10}	1.9×10^{-10}

Table 2. The relevant particle spectrum of the four adopted benchmark points, presented together with the values of several low-energy observables suitable for constraining the model. All of the sleptons given here are RH. The subscripts R and I in sneutrinos refer to real and imaginary parts, respectively. All masses are given in GeV.

channel, as depicted in Fig. 1. For setups where RH neutrinos are lighter than sneutrinos, a t -channel neutralino exchange diagram also exists, although it turns out to be suppressed for heavy neutralinos. We concentrate in this work on scenarios where the RH neutrinos are always heavier than the LSP.

Dark matter relic density and direct detection constraints have been calculated with MADDM v2.0 [48], and we have used MICROMEGAS [49] to validate our findings. Due to the dominance of the relic density on the s -channel diagrams given in Fig. 1, it only depends on the RH sneutrino mass. Existing bounds are found to be satisfied with sneutrinos having

a mass lying in the [250 GeV, 290 GeV] range (provided all co-annihilation channels are negligible). We adjusted the lightest sneutrino mass to lie in this range for our benchmarks. For the exact BP1 and BP2 parameters, we obtain a relic density prediction of $\Omega_{\text{DM}}h^2 = 0.119$ and 0.116 for the BP1 and BP2 point respectively. In addition, the spin-independent cross sections for DM-nucleon scattering is smaller than 2.5×10^{-10} pb for both benchmark scenarios, which agrees with the current bounds.

If the sensitivity of direct detection experiments increases by a factor of three, we should either see a signal or exclude typical benchmarks like BP1 or BP2. As the DM-nucleon scattering is mediated mostly via the SM-like Higgs boson, a direct detection signal will be largely unaffected by the details of the unknown particle spectrum and thus provides a robust way of testing right sneutrino DM in LRSUSY models. In presence of coannihilations or large mixing between the left and right sneutrino sectors, the observed relic density may point to another mass range than in our case. Moreover, if heavier sneutrinos are allowed, the direct detection bounds are weaker and the exclusion will be more difficult.

We observe a remarkable feature originating from the left-right symmetry. By construction, the RH sneutrino fields are a part of $SU(2)_R$ doublets while the SM-like Higgs boson is in contrast originating mainly from the Higgs bidoublets. As the RH neutrino and Higgs bidoublet fields couple very strongly, the annihilation cross section is large enough for ensuring a correct relic density, even if the associated process occurs non-resonantly. The RH sneutrino coupling to the Z -boson is on the other hand weak enough for preventing dark matter annihilation to be too efficient. As a consequence, the only relevant parameters driving the relic density are the $SU(2)_R$ gauge coupling (see Eq. (2.8)) and the LSP mass, so that a correct relic density can be obtained for a broad range of LRSUSY realizations. This drastically differs from cases where RH sneutrinos are gauge-singlet and where a resonant annihilation is needed to guarantee a correct relic density, like in the next-to-minimal supersymmetric standard model (NMSSM) extended with RH neutrinos [50–53], or when the dark matter candidate is a mixture of LH and RH sneutrinos [3, 7, 54, 55]. In both these cases, extra free parameters are available to tune the relic density to match the experimental bounds, in contrast with the LRSUSY setup unless one includes a large left-right mixing in the sneutrino sector.

The main DM annihilation channel proceeding via a Higgs-boson exchange, this consequently implies that the main sneutrino pair-production mode at the LHC will proceed via an s -channel Higgs-boson exchange as well. Typical DM searches relying on initial-state radiation would then be insensitive to this LRSUSY setup, the order of magnitude of the corresponding cross section being at the attobarn level due to a suppression by the weakness of the Higgs interactions with the QCD partons and the non-resonant configuration driven by the Higgs-boson and RH sneutrino mass difference. RH sneutrino are hence dominantly produced from the decay of other particles. One obvious candidate is the heavier MSSM-like Higgs state, but its (gauge) couplings to the sneutrinos whose form is similar to Eq (2.8) vanishes in the alignment limit. The dominant LHC RH sneutrino production mode therefore proceeds via the resonant production of a W_R -boson.

4.2 Neutralino dark matter

LRSUSY neutralino dark matter has been already discussed in the past, but under assumptions different from ours. Ref. [56] considers neutralinos that are pure gauge eigenstates, so that their results must be generalized to the case where neutralinos are admixtures of electroweakinos and higgsinos, whereas Ref. [57] has built a LRSUSY model where $B - L = 0$ Higgs triplets are included and RH Higgs triplets VEVs are decoupled, forbidding the W_R -induced production of pairs of superpartners.

In our LRSUSY parameterization, the composition of the lightest neutralino depends on the soft gaugino masses. We have chosen M_1 to be the smallest gaugino mass parameter to guarantee a bino-dominated LSP, and fix its value in order to obtain a relic density prediction in agreement with data. The M_1 parameter is nonetheless connected to the $U(1)_{B-L}$ gaugino (that we abusively call bino), so that it does not couple to the light gauge bosons and the bidoublet Higgs fields. The bino however mixes with the other gauginos, which ensures non-vanishing couplings to the Z -boson and the SM-like Higgs-boson.

The resulting relic density is in general too large and we need a resonant contribution to increase the DM annihilation cross section. For this reason, our neutralino LSP benchmarks feature a $\tilde{\chi}_1^0$ mass slightly below half the Higgs-boson mass $m_h/2$. The kinematically allowed $h \rightarrow \tilde{\chi}_1^0 \tilde{\chi}_1^0$ decay is suppressed since the LSP is bino-dominated and the bidoublets are not charged under $U(1)_{B-L}$. The corresponding branching ratios for the BP3 and BP4 cases are found to be about 4×10^{-4} , which is of the same order as the SM Higgs-boson invisible branching ratio, and the associated relic density is respectively $\Omega_{\text{DM}} h^2 = 0.107$ and 0.124 for the two benchmark scenarios. Furthermore, the spin-independent and spin-dependent nucleon-DM scattering cross sections are of 3×10^{-11} pb and 2×10^{-6} pb for both benchmark points, which satisfies current direct detection bounds [58].

5 Collider phenomenology at the LHC

5.1 Analysis strategy for discovering LRSUSY at the LHC

In the MSSM, the production of weakly interacting superpartners in proton-proton collisions at a center-of-mass energy of 13 TeV is limited, so that current search limits for sleptons and electroweakinos are weaker than for the strongly interacting sector. These searches additionally rely on a very high LHC luminosity to be sensitive to superparticles lying in the 1 TeV mass regime. Moreover, production cross sections for RH scalar partners are smaller than for LH partners for a given superparticle mass. This is one of the most crucial differences for the LRSUSY case, RH scalar production cross sections being here enhanced thanks to the gauging of the RH sector, on top of the fact that a RH sneutrino can be a good DM candidate.

Right-handed slepton and sneutrino production at the LHC is mediated by heavy RH gauge boson exchanges. The corresponding rates are enhanced if resonant configurations are reached, so that the LHC is possibly sensitive to high mass scales. In this section, we make use of resonant slepton and sneutrino production to show how robust and clean these signals can be and how they can provide handles for pushing the LHC reach for the

	BP1	BP2	BP3	BP4
$\sigma(pp \rightarrow W_R)$ (fb)	245	38	245	38
$\text{BR}(W_R \rightarrow \tilde{\nu}_{I\tau}\tilde{\ell}_\tau)$	0.52%	0.52%	0.38%	0.61%
$\text{BR}(W_R \rightarrow \tilde{\nu}_{Ie}\tilde{\ell}_e)$	0.64%	1.06%	0.80%	0.82%
$\text{BR}(W_R \rightarrow \tilde{\nu}_{I\mu}\tilde{\ell}_\mu)$	0.60%	0.98%	0.57%	0.74%
$\text{BR}(W_R \rightarrow \tilde{\nu}_{Re}\tilde{\ell}_e)$	0.21%	0.60%	0.42%	0.47%
$\text{BR}(W_R \rightarrow \tilde{\nu}_{R\mu}\tilde{\ell}_\mu)$	0.24%	0.47%	0.19%	0.36%
$\sigma \times \sum \text{BR}(W_R \rightarrow \tilde{\nu}\tilde{\ell})$ (fb)	5.4	1.4	5.8	1.1

Table 3. W_R -boson production cross sections for proton-proton collisions at a center-of-mass energy $\sqrt{s} = 13$ TeV, and W_R branching ratios to sleptonic final states.

weakly-interacting sector beyond 1 TeV. We consider the production process

$$pp \rightarrow \sum \tilde{\nu} \tilde{\ell} \quad (5.1)$$

where we sum over all possible final states, *i.e.*, we include three generations of sleptons and of scalar and pseudoscalar RH sneutrinos. We observe that the bulk of the cross section originates from on-shell W_R^\pm production followed by its decays into a slepton-sneutrino final state. Our predictions rely on the UFO libraries [59] outputted by SARAH to generate the relevant hard-scattering matrix elements with MADGRAPH5_aMC@NLO [60]. More precisely, we convolute these matrix elements with the NNPDF 2.3 sets of parton densities [61] to obtain the leading-order cross section values indicated in Table 3, the branching ratios being those returned by SPHENO. We find that the smaller W_R -boson production cross sections for the BP2 and BP4 cases are partly compensated by the larger branching ratios, but will also feature a sleptonic decay phase space configuration where a slightly harder transverse-momentum (p_T) is expected for the heavy gauge boson decay products.

As $\mathcal{O}(100 \text{ fb}^{-1})$ of integrated luminosity can be recorded by the LHC current and future runs, our cross section results show that a fairly reasonable number of signal events could be expected for our typical benchmark scenarios. Slepton production could hence be a promising mode to look for LRSUSY signals provided the SM background could be reduced.

We start with processes in which the lightest sneutrino is produced. For the BP2, BP3 and BP4 scenarios, charged sleptons almost always decay into a charged lepton of the same flavor and a light neutralino $\tilde{\chi}_1^0$. In contrast, in the BP1 scenario, this decay mode only occurs with a probability of about 30% and sleptons mostly decay into a $\ell\tilde{\chi}_5^0$ final state with a branching ratio of 70%. The heavier $\tilde{\chi}_5^0$ neutralino then decays entirely into a final-state system made of a W -boson and the lightest chargino that further decays, with a 100% probability, into the LSP and a tau lepton. When the lightest neutralino $\tilde{\chi}_1^0$ is the LSP for the BP3 and BP4 scenarios, it decays invisibly for the BP2 scenario so that the

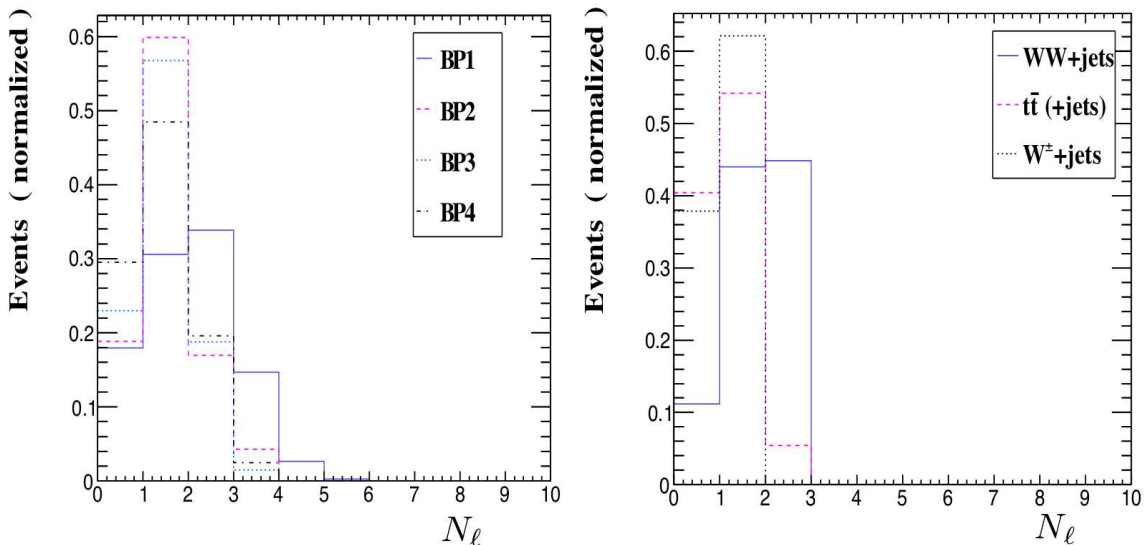


Figure 2. Parton-level charged lepton multiplicity distributions for the LRSUSY signals (left) and for the dominant SM backgrounds (right), all curves being normalised to 1.

three benchmarks will feature a similar signature,

$$\text{BP2} - \text{BP3} - \text{BP4} : \quad pp \rightarrow W_R \rightarrow \sum \tilde{\ell} \tilde{\nu} \rightarrow 1\ell + \cancel{E}_T . \quad (5.2)$$

For the case of the first benchmark scenario, extra signatures have to be considered, in particular as a same-sign dilepton signal could arise due to the Majorana nature of the intermediate $\tilde{\chi}_5^0$ state,

$$\text{BP1} : \quad pp \rightarrow W_R \rightarrow \sum \tilde{\ell} \tilde{\nu} \rightarrow \ell + \cancel{E}_T \quad \text{or} \quad \ell + \tau + W + \cancel{E}_T . \quad (5.3)$$

The golden same-sign dilepton signal however suffers from the low W -boson leptonic branching fraction. On the other hand, heavier sneutrinos produced in association with charged sleptons decay down to a chargino and a charged lepton (e or μ) almost half of the time, which suggests that at least one highly energetic final-state charged electron or muon can be expected in such processes.

For simplicity, we ignore all electronic or muonic tau decays in the rest of our analysis, although τ -enriched final states would be more frequently produced as the sneutrino LSP is of the τ flavor. In Fig. 2 we present the charged lepton multiplicity of the signal that is expected for the different benchmark points (left) as well as for the dominant source SM background (right). The predictions are calculated at the parton level and the results have been normalized to 1. This suggests to consider two possible signal signatures,

$$\begin{aligned} (i) & \quad \geq 1\ell + n j + \cancel{E}_T & \text{with } n \leq 3 , \\ (ii) & \quad \geq 2\ell + n j + \cancel{E}_T & \text{with } n \leq 3 , \end{aligned} \quad (5.4)$$

where $\ell = e^\pm$ or μ^\pm and the constraint on the jet multiplicity originates from the topology of the signal that is poor in final-state jets. Even if appealing, the second LRSUSY signal

handle (ii) may be challenging to use, the associated production rate being expected to suffer from an important suppression relative to the first signature (i). We therefore focus, for this pioneering study, on final-state systems containing one or more charged leptons accompanied by a large amount of missing transverse momentum \cancel{E}_T and a small number of jets. The dominant source of SM background is expected to consist of charged-current Drell-Yan-like production (in association with jets) where typical final-states feature a single hard lepton (as shown in the right panel of Fig. 2) and missing energy carried by the final-state neutrino. Top quark-antiquark pair production also contributes when leptonic top quark decays are considered, as well as various diboson production channels that traditionally give rise to lepton-enriched final-states featuring missing energy as well. Neutral current Drell-Yan events could in principle contribute, but the corresponding final-state does not usually exhibit a large amount of missing energy so that it can be rejected quite strongly with an appropriate missing energy selection, such as the one performed in our analysis (see below). We have also verified that triboson contributions are negligible after event selection, so that both the neutral-current Drell-Yan-like and triboson processes have been omitted from our simulation.

Signal and background hard scattering events have been generated at the leading-order accuracy with the MADGRAPH5_aMC@NLO program, using the NNPDF 2.3 parton density sets, and matched with the parton shower infrastructure and hadronization framework of PYTHIA 8.2 [62]. Our simulation strategy furthermore follows the MLM merging scheme [63] for combining event samples featuring a different jet multiplicity. We have simulated the response of an LHC-like detector by employing the DELPHES 3.0 program [64] and finally reconstructed all final-state jets by means of the anti- k_T algorithm [65] as embedded into FASTJET [66].

The transverse momentum p_T^ℓ and pseudorapidity η^ℓ of all electron and muon candidates are required to satisfy

$$p_T^\ell > 20 \text{ GeV} \quad \text{and} \quad |\eta^\ell| < 2.5 , \quad (5.5)$$

and we consider jet candidates whose transverse momentum p_T^j and pseudorapidity η^j fulfill

$$p_T^j > 40 \text{ GeV} \quad \text{and} \quad |\eta_j| < 2.5 . \quad (5.6)$$

We have moreover imposed that all reconstructed objects are isolated from each other in the transverse plane, their angular distance ΔR being required to be larger than 0.4 (0.5 in the case of two jets). In order to optimize the selection to push the signal-to-noise ratio to a large level, we use the MADANALYSIS 5 software [67] to implement our phenomenological analysis. We require the presence of at least one reconstructed lepton and at most three reconstructed jets,

$$N_\ell \geq 1 \quad \text{and} \quad N_j \leq 3 , \quad (5.7)$$

and constrain the amount of transverse missing energy to satisfy

$$\cancel{E}_T > 200 \text{ GeV} . \quad (5.8)$$

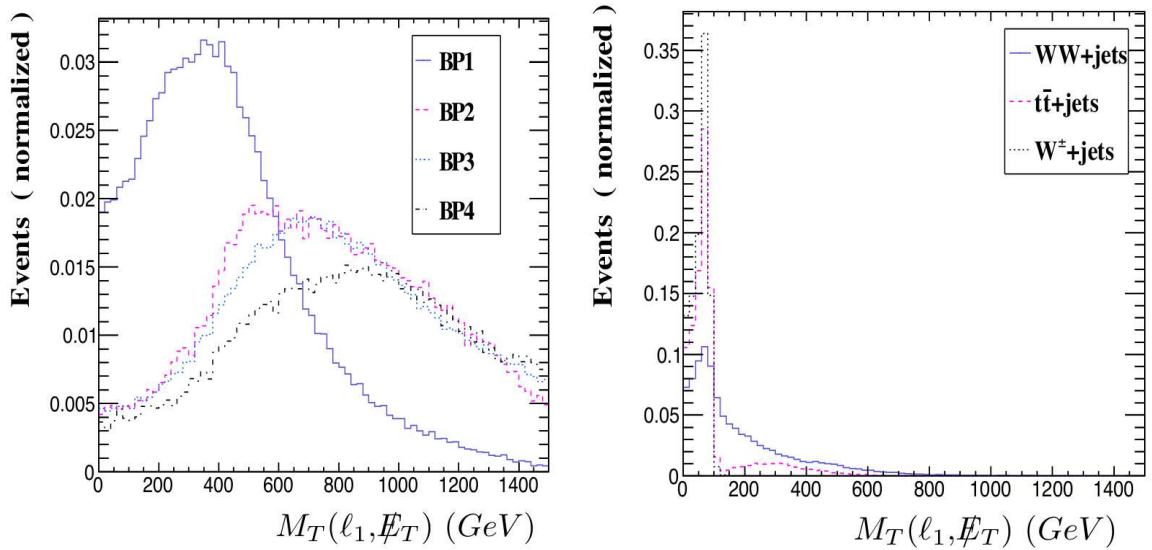


Figure 3. Distribution in the transverse mass M_T of the leading lepton and the missing transverse momentum for the different benchmark point signals (left) and for the SM background (right). The distributions are shown after the basic acceptance selections defined in the text and normalized to 1.

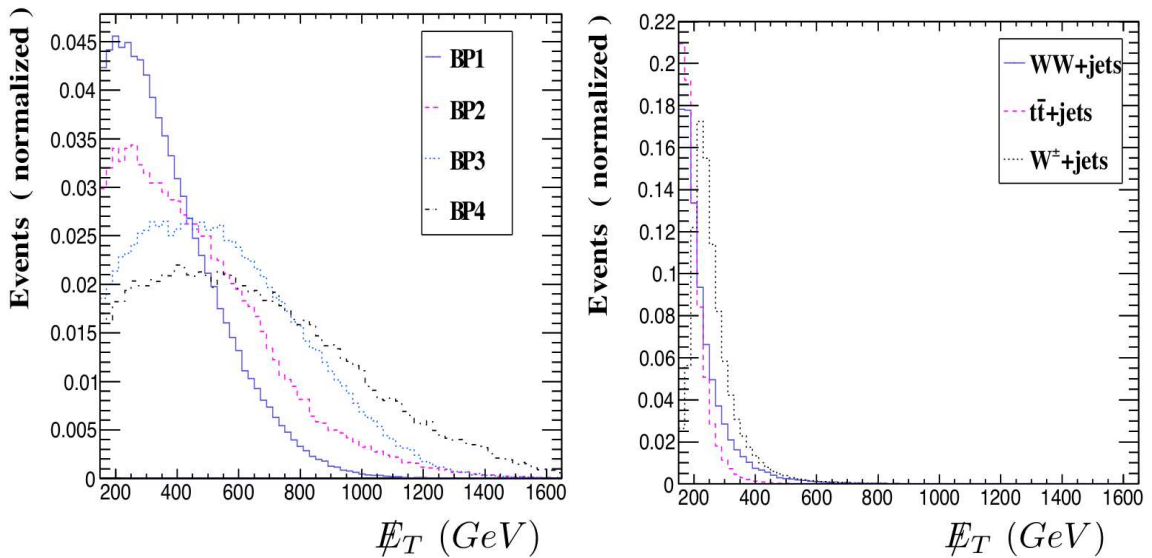


Figure 4. Same as in Fig. 3 but for the missing transverse energy E_T .

We moreover veto all events featuring either isolated photons with a p_T greater than 10 GeV or b -tagged jets, using b -tagging efficiencies and mis-tagging rates typical of the CMS detector (and implemented in the DELPHES detector parameterization). The above selections allow us to reduce all backgrounds (the b -tagged jet requirement specifically aiming to reduce the $t\bar{t}$ background) to a large extent while maintaining a signal efficiency of about 50%.

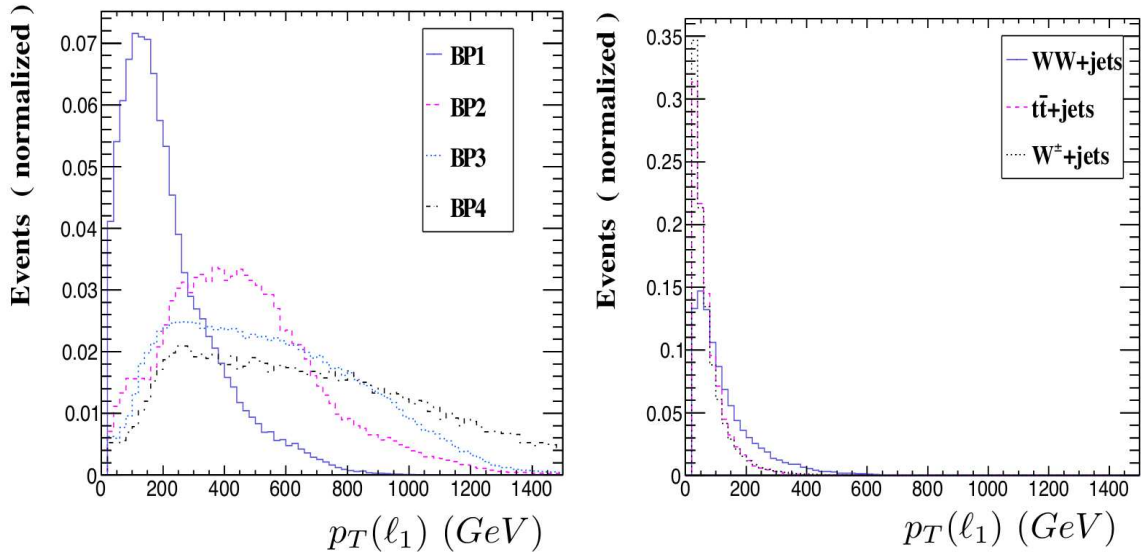


Figure 5. Same as in Fig. 3 but for the transverse momentum of the leading lepton.

The largest background contribution comes at this stage from charged-current Drell-Yan-like events and still overwhelms the signal. The latter however features leptons and missing energy originating from the decay of very massive superpartners. This can be used to design an appropriate selection, relying on, *e.g.*, the transverse mass $M_T(\ell_1, \cancel{E}_T)$ of the system made of the leading lepton and the missing transverse energy. This observable is represented in Fig. 3 for both the four signal benchmark scenarios (left) and the backgrounds (right) after that all the previous selections have been applied. We additionally compare the signal and background distributions in the missing transverse momentum (Fig. 4) and in the transverse momentum $p_T(\ell_1)$ of the leading lepton (Fig. 5). This demonstrates that all these three observables yield neat handles for enhancing the signal over background ratio, the signal spectra for each case being much harder than the background ones. Analyzing the signal only, we observe that the distributions are harder for the BP3 and BP4 scenarios than for the BP1 and BP2 scenarios. This results from the superparticle spectrum associated with these scenarios (see Table 2), which features an important mass gap between the light LSP and the charged sleptons that decay into the LSP and the corresponding lepton. This contrasts with the BP1 and BP2 benchmarks where leptons also originates from slepton decays, but where there is not such a large mass gap with the LSP. From the above considerations, we impose a set of three selections,

$$\cancel{E}_T > 250 \text{ GeV}, \quad M_T(\ell_1, \cancel{E}_T) > 250 \text{ GeV} \quad \text{and} \quad p_T(\ell_1) > 100 \text{ GeV} \quad \text{for} \quad \ell = e, \mu, \quad (5.9)$$

which yields to an important background rejection, as illustrated in Table 4 for an integrated luminosity of 100 fb^{-1} .

The LHC turns out to be sensitive to the BP3 and BP1 scenarios that feature a lighter W_R boson with a mass of about 2.7 TeV with a statistical significance of 11σ and 5σ respectively. Although the BP2 and BP4 scenarios suffer from the reduction of the signal

	BP1	BP2	BP3	BP4	diboson	top-antitop	Drell-Yan
Preselection	216	83	299	45	2065	7192	5.94×10^5
$M_T(\ell_1, \cancel{E}_T) > 250$ GeV	153	77	279	42	521	708	142
$p_T(\ell_1) > 100$ GeV	134	75	274	42	440	559	124
$\cancel{E}_T > 250$ GeV	113	67	258	40	229	149	69

Table 4. Number of events surviving each step of our selection strategy for the four signal benchmark scenarios and the three main background components. We assume an integrated luminosity of 100 fb^{-1} .

	BP1	BP2	BP3	BP4	diboson	top-antitop
$n_\ell \geq 2; p_T(\ell_1) > 200$ GeV	55	21	77	14	94	50
$p_T(\ell_2) > 40$ GeV	50	18	66	13	72	38
$M_T(\ell_2, \cancel{E}_T) > 50$ GeV	46	17	63	13	41	21

Table 5. Number of events surviving each step of a typical LRSUSY selection targetting the signature (ii) of Eq. (5.4). We assume (and omit), as a preselection, the analysis depicted in Table 4.

cross section induced by the W_R -boson mass of about 3.5 TeV, significances of 3σ and 1.86σ are obtained. As evident from Fig. 5, the BP2, BP3 and BP4 benchmarks implies a $p_T(\ell_1)$ distribution that is very hard, as expected from the decay pattern of Eq. (5.2), which provides an extra way to increase the significance. For example, a selection of 200 GeV on the leading slepton transverse momentum would suppress the total number of background events to 250, for an integrated luminosity of 100 fb^{-1} , whereas the number of signal events drops to 72, 63, 235 and 38 for the BP1, BP2, BP3 and BP4 scenarios respectively. This improves the significance for BP4 to about 2.3σ . Our analysis hence clearly suggests that LRSUSY sleptons with masses of around 800 GeV could be accessible at the current run of the LHC with a luminosity that is as low as 50 fb^{-1} , provided the W_R -boson mass is around 3 TeV.

We have verified that for the second signature of Eq. (5.4), there is a marked suppression in the number of selected signal events, so that any potentially visible excess would require a significantly higher integrated luminosity. The impact of a typical analysis strategy is shown in Table 5, the selection requiring the presence of at least two charged leptons. The second lepton is constrained to be harder than 40 GeV and the transverse mass for this second lepton and the missing momentum is required to be larger than 50 GeV.

5.2 Collider consequences of the LSP nature in LRSUSY models

For LRSUSY scenarios with a bino-dominated LSP, charged sleptons and sneutrinos both decay into the neutralino LSP and either a lepton or a RH neutrino with a large branching fraction. The RH neutrino then decays into an ℓjj system so that the full decay chain is connected with a signature that includes two leptons, two jets and missing transverse energy. In the case where sneutrinos cannot decay into a $\nu_R \tilde{\chi}_1^0$ final state, they instead decay invisibly to a $\nu_L \tilde{\chi}_1^0$ system which does not yield any multileptonic final state. As a result of the decay tables of our benchmarks, decay modes exhibiting three or more leptons are rare and the corresponding number of events amounts to about 10% of the number of dilepton events. The situation is slightly different for scenarios where the LSP is a sneutrino. One expects lepton-enriched final states, as intermediate charginos that can be produced in the longer decay chains lead to additional leptons (like for the BP1 point). In this case, the number of events featuring three leptons amounts to 20 – 30% of the number of expected dilepton events. With a luminosity of 100 fb^{-1} , this number is however too small to get any statistically-significant way to distinguish a sneutrino LSP scenario from the corresponding neutralino LSP scenario. However, there is hope for the high-luminosity phase of the LHC, as for the study of the rarer same-sign dilepton signature that seems very unlikely to yield any visible signals at the low-luminosity phase of the LHC.

LRSUSY sneutrino LSP scenarios present also a very different phenomenology from the corresponding MSSM scenarios where the MSSM is extended by RH neutrino superfields. In this last case, the Lagrangian includes Dirac mass terms for the neutrinos and the lightest stau is often close in mass to the sneutrino. Due to the small associated Yukawa coupling, the lightest stau is long-lived [68], which contrasts with our scenarios where the stau is much heavier than the sneutrinos (see Eqs. (2.11), (2.14) and (2.15)). In LRSUSY, the next-to-lightest superpartner (NLSP) turns thus out to be another particle, and the presence of larger couplings of the sneutrino to the other particles guarantees that the NLSP is typically not long-lived.

The LHC is expected in general to be more sensitive to LRSUSY realizations with a sneutrino LSP than for MSSM setups with a RH neutrino. Equivalently, higher superpartner masses could be reached. In the MSSM, multileptonic final states arise from electroweakino decays that can be either directly produced or indirectly produced from squark and gluino decays [55, 69, 70]. The production rate of electroweakinos with masses lying beyond 1 TeV is however small, whereas the presence of the RH gauge sector in LRSUSY enhances it, at least if the W_R -boson mass is not much greater than 3 TeV. Corresponding events feature, in addition, a larger amount of missing transverse momentum and at least one very hard lepton, which helps to suppress the SM background.

6 Summary and conclusions

In this work we investigated the phenomenology of right-sneutrinos in LRSUSY models. The RH neutrino superfields being part of a doublet, the expectations are different from those of models with singlet neutrino superfields. We studied the impact of having an LSP RH sneutrino and shown that it could be a viable DM candidate satisfying all cosmological

constraints. In particular, the DM annihilation cross section does not need any specific enhancement to accommodate the relic abundance observations. The only coupling responsible for DM annihilation in the early Universe is a gauge coupling and there is a wide range of sneutrino masses yielding a correct relic density.

We devised four benchmarks for our comparative study of LRSUSY scenarios with a sneutrino and with a neutralino LSP, two benchmarks featuring a right-sneutrino LSP, and two a neutralino LSP. We considered two values of the W_R -boson mass, chosen to agree with limits stemming from dijet measurements at the LHC. In addition, the benchmarks have been imposed to satisfy dark matter constraints, experimental mass limits and the measurements of several low-energy observables.

We investigated the LHC phenomenology of our LRSUSY scenarios, focusing on a LRSUSY signal originating from resonant slepton production via a W_R -boson exchange and containing one or more charged leptons and missing transverse momentum. For optimistic scenarios with a light W_R boson whose mass is 2.7 TeV, we have shown that the transverse mass of the lepton/missing momentum systems, the missing transverse energy and the transverse momenta of the final-state leptons are suitable observables to differentiate the signal from the background even with a low LHC luminosity of 100 fb^{-1} , both for scenarios with a sneutrino and with a neutralino LSP. For benchmarks with a heavier W_R boson with a mass equal to 3.5 TeV, the discovery of the signal would require a slightly higher integrated luminosity, which the LHC should be able to attain within a few years of running.

Turning to signatures featuring more than two leptons, we have found that the associated signal rates are lower than the dilepton one by about 20-30%. This contrasts with neutralino LSP scenarios where this number goes down to about 10%. Using these probes for distinguishing different LRSUSY setups therefore requires the high-luminosity phase of the LHC. Sneutrino LSP in left-right supersymmetry scenarios also reveal significant differences with sneutrino LSP setups in supersymmetric realizations where the MSSM is extended by a gauge-singlet neutrino superfield. The mass difference between the stau and the sneutrino is larger in LRSUSY, and the stau here is in general neither the NLSP, nor long-lived.

Considering right sneutrino as the DM candidate in LRSUSY realizations presents novel features in the particle spectrum, the corresponding dark matter analysis and the subsequent collider signals. In particular, we propose that a resonantly-enhanced slepton production cross section, otherwise overlooked in typical LRSUSY signals, allows for an improved sensitivity to heavier slepton searches at the LHC. This also constitutes a promising supersymmetric signal of physics beyond the MSSM.

Acknowledgments

The authors would like to thank Arindam Chatterjee for taking part to the initial discussions of this work, Manuel Krauss for providing the LRSUSY SPHENO code and Mihailo Backovic for his help with MADDM. MF thanks the NSERC for partial financial support under grant number SAP105354, KH and HW acknowledge support from the H2020-MSCA-RICE-2014 grant number 645722 (NonMinimalHiggs), the work of SKR has been

partially supported by funding available from the Department of Atomic Energy, Government of India, for the Regional Centre for Accelerator-based Particle Physics (RECAPP) at the Harish-Chandra Research Institute, and BF has been supported in part by French state funds managed by the Agence Nationale de la Recherche (ANR), in the context of the LABEX ILP (ANR-11-IDEX-0004-02, ANR-10-LABX-63).

References

- [1] G. Aad *et al.* (ATLAS Collaboration), Phys. Lett. B **716** (2012) 1, arXiv:1207.7214 [hep-ex].
- [2] S. Chatrchyan *et al.* (CMS Collaboration), Phys. Lett. B **716**, 30 (2012), arXiv:1207.7235 [hep-ex].
- [3] N. Arkani-Hamed, L. J. Hall, H. Murayama, D. Tucker-Smith and N. Weiner, Phys. Rev. D **64**, 115011 (2001), hep-ph/0006312.
- [4] F. Borzumati and Y. Nomura, Phys. Rev. D **64**, 053005 (2001), hep-ph/0007018.
- [5] G. Hinshaw *et al.* (WMAP Collaboration), Astrophys. J. Suppl. **208**, 19 (2013), arXiv:1212.5226 [astro-ph.CO].
- [6] P. A. R. Ade *et al.* (Planck Collaboration), Astron. Astrophys. **594** (2016) A13, arXiv:1502.01589 [astro-ph.CO].
- [7] G. Belanger, M. Kakizaki, E. K. Park, S. Kraml and A. Pukhov, JCAP **1011**, 017 (2010); M. Kakizaki, E. K. Park, J. h. Park and A. Santa, Phys. Lett. B **749**, 44 (2015); A. Chatterjee and N. Sahu, Phys. Rev. D **90**, no. 9, 095021 (2014); B. Dumont, G. Belanger, S. Fichet, S. Kraml and T. Schwetz, JCAP **1209**, 013 (2012); G. Belanger, M. Kakizaki, E. K. Park, S. Kraml and A. Pukhov, JCAP **1011**, 017 (2010); S. Banerjee, G. Belanger, B. Mukhopadhyaya and P. D. Serpico, JHEP **1607**, 095 (2016); C. Arina, M. E. C. Catalan, S. Kraml, S. Kulkarni and U. Laa, JHEP **1505**, 142 (2015) J. A. Evans and J. Shelton, JHEP **1604**, 056 (2016); C. Arina and M. E. Cabrera, JHEP **1404**, 100 (2014); K. Y. Choi and O. Seto, Phys. Rev. D **86**, 043515 (2012) Erratum: [Phys. Rev. D **86**, 089904 (2012)]; K. Ishiwata, M. Kawasaki, K. Kohri and T. Moroi, Phys. Lett. B **689**, 163 (2010); R. Allahverdi, S. Bornhauser, B. Dutta and K. Richardson-McDaniel, Phys. Rev. D **80**, 055026 (2009).
- [8] H. An, P. S. B. Dev, Y. Cai and R. N. Mohapatra, Phys. Rev. Lett. **108**, 081806 (2012).
- [9] S. L. Chen and Z. Kang, Phys. Lett. B **761**, 296 (2016); S. Banerjee, P. S. B. Dev, S. Mondal, B. Mukhopadhyaya and S. Roy, JHEP **1310**, 221 (2013); C. A. de S. Pires, P. S. Rodrigues da Silva, A. C. O. Santos and C. Siqueira, Phys. Rev. D **94**, no. 5, 055014 (2016); W. Abdallah, J. Fiaschi, S. Khalil and S. Moretti, Phys. Rev. D **92**, 055029 (2015); K. Huitu, J. Laamanen, L. Leinonen, S. K. Rai and T. Ruppell, JHEP **1211**, 129 (2012); V. De Romeri and M. Hirsch, JHEP **1212**, 106 (2012); P. S. Bhupal Dev, S. Mondal, B. Mukhopadhyaya and S. Roy, JHEP **1209**, 110 (2012); D. A. Demir, L. L. Everett, M. Frank, L. Selbuz and I. Turan, Phys. Rev. D **81**, 035019 (2010); D. G. Cerdeno and O. Seto, JCAP **0908**, 032 (2009); F. Deppisch and A. Pilaftsis, JHEP **0810**, 080 (2008). C. Arina and N. Fornengo, JHEP **0711**, 029 (2007); H. S. Lee, K. T. Matchev and S. Nasri, Phys. Rev. D **76**, 041302 (2007); T. Asaka, K. Ishiwata and T. Moroi, Phys. Rev. D **75**, 065001 (2007); S. Gopalakrishna, A. de Gouvea and W. Porod, JCAP **0605**, 005 (2006); T. Asaka, K. Ishiwata and T. Moroi, Phys. Rev. D **73**, 051301 (2006); D. Hooper, J. March-Russell and S. M. West, Phys. Lett. B **605**, 228 (2005); T. Han and R. Hempfling,

- Phys. Lett. B **415**, 161 (1997); T. Falk, K. A. Olive and M. Srednicki, Phys. Lett. B **339**, 248 (1994). G. Bélanger, J. Da Silva, U. Laa and A. Pukhov, JHEP **1509**, 151 (2015); B. Dumont, G. Belanger, S. Fichet, S. Kraml and T. Schwetz, JCAP **1209**, 013 (2012) P. Bandyopadhyay, E. J. Chun and J. C. Park, JHEP **1106**, 129 (2011). W. Abdallah and S. Khalil, arXiv:1701.04436 [hep-ph].
- [10] R. N. Mohapatra and G. Senjanovic, Phys. Rev. Lett. **44**, 912 (1980); R. N. Mohapatra and G. Senjanovic, Phys. Rev. D **23** (1981) 165.
- [11] R. M. Francis, M. Frank and C. S. Kalman, Phys. Rev. D **43**, 2369 (1991); K. Huitu, J. Maalampi and M. Raidal, Phys. Lett. B **328**, 60 (1994); K. Huitu, J. Maalampi and M. Raidal, Nucl. Phys. B **420**, 449 (1994); C. S. Aulakh, A. Melfo and G. Senjanovic, Phys. Rev. D **57**, 4174 (1998).
- [12] R. N. Mohapatra and A. Rasin, Phys. Rev. Lett. **76**, 3490 (1996); R. N. Mohapatra and A. Rasin, Phys. Rev. D **54**, 5835 (1996); R. Kuchimanchi, Phys. Rev. Lett. **76**, 3486 (1996).
- [13] K. S. Babu and R. N. Mohapatra, Phys. Lett. B **668**, 404 (2008); M. Frank and B. Korutlu, Phys. Rev. D **83**, 073007 (2011).
- [14] M. Frank, D. K. Ghosh, K. Huitu, S. K. Rai, I. Saha and H. Waltari, Phys. Rev. D **90**, no. 11, 115021 (2014).
- [15] C. S. Aulakh, A. Melfo, A. Rasin and G. Senjanovic, Phys. Rev. D **58**, 115007 (1998); C. S. Aulakh, K. Benakli and G. Senjanovic, Phys. Rev. Lett. **79**, 2188 (1997); M. Hirsch, M. E. Krauss, T. Opferkuch, W. Porod and F. Staub, JHEP **1603**, 009 (2016).
- [16] R. N. Mohapatra, A. Rasin and G. Senjanovic, Phys. Rev. Lett. **79** (1997) 4744, hep-ph/9707281.
- [17] A. Alloul, M. Frank, B. Fuks and M. Rausch de Traubenberg, JHEP **1310** (2013) 033, arXiv:1307.5073 [hep-ph].
- [18] W. Porod and F. Staub, Comput. Phys. Commun. **183** (2012) 2458, arXiv:1104.1573 [hep-ph].
- [19] F. Staub, Comput. Phys. Commun. **185** (2014) 1773, arXiv:1309.7223 [hep-ph].
- [20] L. Basso, B. Fuks, M. E. Krauss and W. Porod, JHEP **1507** (2015) 147, arXiv:1503.08211 [hep-ph].
- [21] R. Kuchimanchi and R. N. Mohapatra, Phys. Rev. Lett. **75** (1995) 3989, hep-ph/9509256.
- [22] K. S. Babu and A. Patra, Phys. Rev. D **93** (2016) no.5, 055030, arXiv:1412.8714 [hep-ph].
- [23] S. Chatrchyan *et al.* (CMS Collaboration), Phys. Lett. B **718** (2013) 1229, arXiv:1208.0956 [hep-ex].
- [24] S. Chatrchyan *et al.* (CMS Collaboration), Phys. Rev. Lett. **109** (2012) 261802, arXiv:1210.2402 [hep-ex].
- [25] V. Khachatryan *et al.* (CMS Collaboration), Eur. Phys. J. C **74** (2014) no.11, 3149, arXiv:1407.3683 [hep-ex].
- [26] G. Aad *et al.* (ATLAS Collaboration), Phys. Lett. B **754** (2016) 302, arXiv:1512.01530 [hep-ex].
- [27] A. M. Sirunyan *et al.* (CMS Collaboration), arXiv:1611.03568 [hep-ex]; G. Aad *et al.* (ATLAS Collaboration), ATLAS-CONF-2016-069.

- [28] M. Aaboud *et al.* (ATLAS Collaboration), Phys. Lett. B **761** (2016) 372, arXiv:1607.03669 [hep-ex].
- [29] V. Khachatryan *et al.* (CMS Collaboration), Phys. Lett. B **768** (2017) 57, arXiv:1609.05391 [hep-ex].
- [30] U. Egede, M. Wielers and M. Peterson, ATL-PHYS-97-097, ATL-GE-PN-97, CERN-ATL-PHYS-97-097.
- [31] S. Chatrchyan *et al.* (CMS Collaboration), Eur. Phys. J. C **72** (2012) 2189, arXiv:1207.2666 [hep-ex].
- [32] CMS Collaboration, CMS-PAS-HIG-14-039.
- [33] CMS Collaboration, CMS-PAS-HIG-16-036.
- [34] K. S. Babu and S. Jana, Phys. Rev. D **95** (2017) no.5, 055020, arXiv:1612.09224 [hep-ph].
- [35] Z. Chacko and R. N. Mohapatra, Phys. Rev. D **58**, 015003 (1998), hep-ph/9712359.
- [36] B. Dutta and R. N. Mohapatra, Phys. Rev. D **59**, 015018 (1999), hep-ph/9804277.
- [37] D. A. Demir, M. Frank, K. Huitu, S. K. Rai and I. Turan, Phys. Rev. D **78**, 035013 (2008), arXiv:0805.4202 [hep-ph].
- [38] D. A. Demir, M. Frank, D. K. Ghosh, K. Huitu, S. K. Rai and I. Turan, Phys. Rev. D **79**, 095006 (2009), arXiv:0903.3955 [hep-ph].
- [39] K. S. Babu, A. Patra and S. K. Rai, Phys. Rev. D **88**, 055006 (2013), arXiv:1306.2066 [hep-ph].
- [40] A. Alloul, M. Frank, B. Fuks and M. Rausch de Traubenberg, Phys. Rev. D **88**, 075004 (2013), arXiv:1307.1711 [hep-ph].
- [41] K. S. Babu, X. G. He and E. Ma, Phys. Rev. D **36** (1987) 878.
- [42] V. Khachatryan *et al.* (CMS Collaboration), JHEP **1410** (2014) 160, arXiv:1408.3316 [hep-ex].
- [43] M. Aaboud *et al.* (ATLAS Collaboration), Eur. Phys. J. C **76** (2016) no.11, 585, arXiv:1608.00890 [hep-ex].
- [44] T. Saito *et al.* (Belle Collaboration), Phys. Rev. D **91** (2015) no.5, 052004, arXiv:1411.7198 [hep-ex].
- [45] T. Hermann, M. Misiak and M. Steinhauser, JHEP **1211** (2012) 036, arXiv:1208.2788 [hep-ph].
- [46] W. Y. Keung and G. Senjanovic, Phys. Rev. Lett. **50** (1983) 1427.
- [47] P. Achard *et al.* (L3 Collaboration), Phys. Lett. B **517** (2001) 75, hep-ex/0107015.
- [48] M. Backovic, A. Martini, O. Mattelaer, K. Kong and G. Mohlabeng, Phys. Dark Univ. **9-10** 37, arXiv:1505.04190 [hep-ph].
- [49] G. Belanger, F. Boudjema, A. Pukhov and A. Semenov, Comput. Phys. Commun. **192** (2015) 322, arXiv:1407.6129 [hep-ph].
- [50] D. G. Cerdeno, C. Munoz and O. Seto, Phys. Rev. D **79** (2009) 023510, arXiv:0807.3029 [hep-ph].
- [51] D. G. Cerdeno and O. Seto, JCAP **0908** (2009) 032, arXiv:0903.4677 [hep-ph].

- [52] A. Chatterjee, D. Das, B. Mukhopadhyaya and S. K. Rai, JCAP **1407**, 023 (2014), arXiv:1401.2527 [hep-ph].
- [53] D. G. Cerdeno, M. Peiro and S. Robles, JCAP **1408** (2014) 005, arXiv:1404.2572 [hep-ph].
- [54] C. Arina and N. Fornengo, JHEP **0711** (2007) 029, arXiv:0709.4477 [hep-ph].
- [55] C. Arina, M. E. C. Catalan, S. Kraml, S. Kulkarni and U. Laa, JHEP **1505** (2015) 142, arXiv:1503.02960 [hep-ph].
- [56] D. A. Demir, M. Frank and I. Turan, Phys. Rev. D **73** (2006) 115001, hep-ph/0604168.
- [57] J. N. Esteves, J. C. Romao, M. Hirsch, W. Porod, F. Staub and A. Vicente, JHEP **1201** (2012) 095, arXiv:1109.6478 [hep-ph].
- [58] D. S. Akerib *et al.* (LUX Collaboration), Phys. Rev. Lett. **118** (2017) no.2, 021303, arXiv:1608.07648 [astro-ph.CO].
- [59] C. Degrande, C. Duhr, B. Fuks, D. Grellscheid, O. Mattelaer and T. Reiter, Comput. Phys. Commun. **183**, 1201 (2012), arXiv:1108.2040 [hep-ph].
- [60] J. Alwall *et al.*, JHEP **1407** (2014) 079, arXiv:1405.0301 [hep-ph].
- [61] R. D. Ball *et al.* (NNPDF Collaboration), JHEP **1504**, 040 (2015), arXiv:1410.8849 [hep-ph].
- [62] T. Sjöstrand *et al.*, Comput. Phys. Commun. **191**, 159 (2015), arXiv:1410.3012 [hep-ph].
- [63] M. L. Mangano, M. Moretti, F. Piccinini and M. Treccani, JHEP **0701**, 013 (2007), hep-ph/0611129.
- [64] J. de Favereau *et al.* (DELPHES 3 Collaboration), JHEP **1402**, 057 (2014), arXiv:1307.6346 [hep-ex].
- [65] M. Cacciari, G. P. Salam and G. Soyez, JHEP **0804** (2008) 063, arXiv:0802.1189 [hep-ph].
- [66] M. Cacciari, G. P. Salam and G. Soyez, Eur. Phys. J. C **72** (2012) 1896, arXiv:1111.6097 [hep-ph].
- [67] E. Conte, B. Fuks and G. Serret, Comput. Phys. Commun. **184**, 222 (2013), arXiv:1206.1599 [hep-ph].
- [68] S. K. Gupta, B. Mukhopadhyaya and S. K. Rai, Phys. Rev. D **75**, 075007 (2007), hep-ph/0701063.
- [69] C. Arina and M. E. Cabrera, JHEP **1404** (2014) 100, arXiv:1311.6549 [hep-ph].
- [70] S. Banerjee, G. Bélanger, B. Mukhopadhyaya and P. D. Serpico, JHEP **1607** (2016) 095, arXiv:1603.08834 [hep-ph].